Supplement of Biogeosciences, 12, 2063–2076, 2015
http://www.biogeosciences.net/12/2063/2015/
doi:10.5194/bg-12-2063-2015-supplement

Biogeosciences Open Access

Supplement of

Numerical analysis of the primary processes controlling oxygen dynamics on the Louisiana shelf

L. Yu et al.

Correspondence to: L. Yu (liuqian.yu@dal.ca)

Online Supplement for Yu et al. "Numerical analysis of the primary processes controlling oxygen dynamics on the Louisiana Shelf"

Table S1. Parameters and parameter values of the biological model.

Symbol	Description	Value	Unit
	Nutrients		
n_{max}	Maximum nitrification rate	0.2	d^{-1}
k_E	Light intensity for half-saturated nitrification inhibition	0.1	$W\ m^{-2}$
E_0	Threshold for light-inhibition of nitrification	0.0095	$W\ m^{-2}$
	Phytoplankton		
μ_0	Phytoplankton growth rate at 0 ℃	0.59	d^{-1}
α	Initial slope of P-I curve	0.025	$mg\ C(mg\ Chl\ W\ m^{-2}d)^{-1}$
k_{NO_3}	Half saturation concentration for nitrate	0.5	$mmol\ N\ m^{-3}$
k_{NH_4}	Half saturation concentration for ammonium	0.5	$mmol\ N\ m^{-3}$
k_{PO_4}	Half saturation concentration for phosphate	0.03	$mmol\ P\ m^{-3}$
m_P	Phytoplankton mortality	0.15	d^{-1}
τ	Phytoplankton and suspended detritus aggregation rate	0.01	$(mmol\ N\ m^{-3})^{-1}d^{-1}$
θ_{max}	Maximum chlorophyll to phytoplankton ratio	0.0535	$mg\ Chl\ mg\ C^{-1}$
w_{Phy}	Sinking velocity of phytoplankton ratio	0.1	$m\ d^{-1}$
	Zooplankton		
g_{max}	Maximum grazing rate	0.6	d^{-1}
k_P	Phytoplankton ingestion half-saturation concentration	2	$(mmol\ N\ m^{-3})^2$
β	Assimilation efficiency	0.75	Dimensionless
l_{BM}	Excretion rate due to basal metabolism	0.1	d^{-1}
l_E	Maximum rate of assimilation related excretion	0.1	d^{-1}
m_Z	Zooplankton mortality	0.025	$(mmol\ N\ m^{-3})^{-1}d^{-1}$
	Detritus		
r_{SD}	Remineralization rate of suspended detritus	0.3	d^{-1}
r_{LD}	Remineralization rate of large detritus	0.01	d^{-1}
r_{RD}	Remineralization rate of river detritus	0.03	d^{-1}
w_{SDet}	Sinking velocity of suspended detritus	0.1	$m\ d^{-1}$
w_{LDet}	Sinking velocity of large particles	5	$m\ d^{-1}$
r_{ox}	Yield of POM oxidation to ammonium in sediments	0.25	$mol\ N\ mol\ N^{-1}$

I. Simulated oxygen budget and hypoxia by normal model simulation

Table S2. Simulated 4-year (2004-2007) mean oxygen budget in summer for the four sub-regions. Oxygen source and sink terms are given for the surface layer above the pycnocline, for the mid layer and for the 5-m thick bottom layer.

Layers	O_2 flux	Mississippi Delta	Mississippi Intermediate	Atchafalaya Plume	Mid-shelf	All regions
	Airsea	-21.2	-10.0	-12.2	-4.8	-11.3
	PP	85.1	68.9	94.8	79.3	79.7
	WR	56.9	55.7	59.6	67.1	60.2
Surface	PP-WR	28.2	13.3	35.2	12.1	19.5
	H+Vadv	-7.8	-4.1	-12.0	-11.6	-8.5
	Vdiff	-5.5	-5.8	-21.1	-5.4	-7.8
	Net	-6.3	-6.6	-10.1	-9.7	-8.0
	PP	65.4	55.3	44.4	61.8	58.1
	WR	61.3	45.6	38.7	55.9	51.5
Mid	PP-WR	4.1	9.7	5.7	5.9	6.7
	H+Vadv	4.8	2.3	1.5	8.3	4.7
	Vdiff	-7.0	-11.5	-2.0	-14.7	-10.1
	Net	2.0	0.5	5.3	-0.4	1.2
	PP	13.6	19.6	23.9	8.7	15.4
	WR	14.1	19.2	35.3	11.1	17.8
	SOC	37.0	39.8	42.8	36.0	38.4
Bottom	PP-WR-SOC	-37.5	-39.4	-54.2	-38.5	-40.8
	H+Vadv	21.2	16.4	13.2	14.4	16.4
	Vdiff	12.4	17.3	23.1	20.1	17.9
	Net	-3.9	-5.7	-17.8	-4.0	-6.5

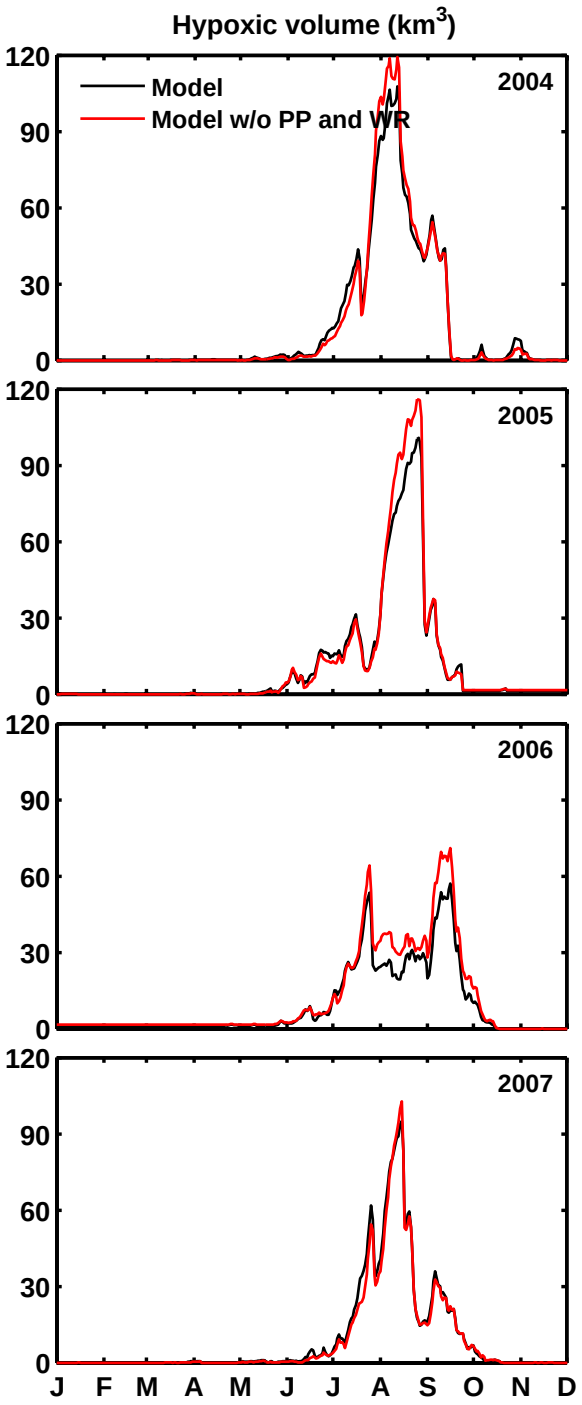

Fig. S1. Time series of simulated hypoxic volume for the full model (black line) and the model without biological processes in the water column (red line).

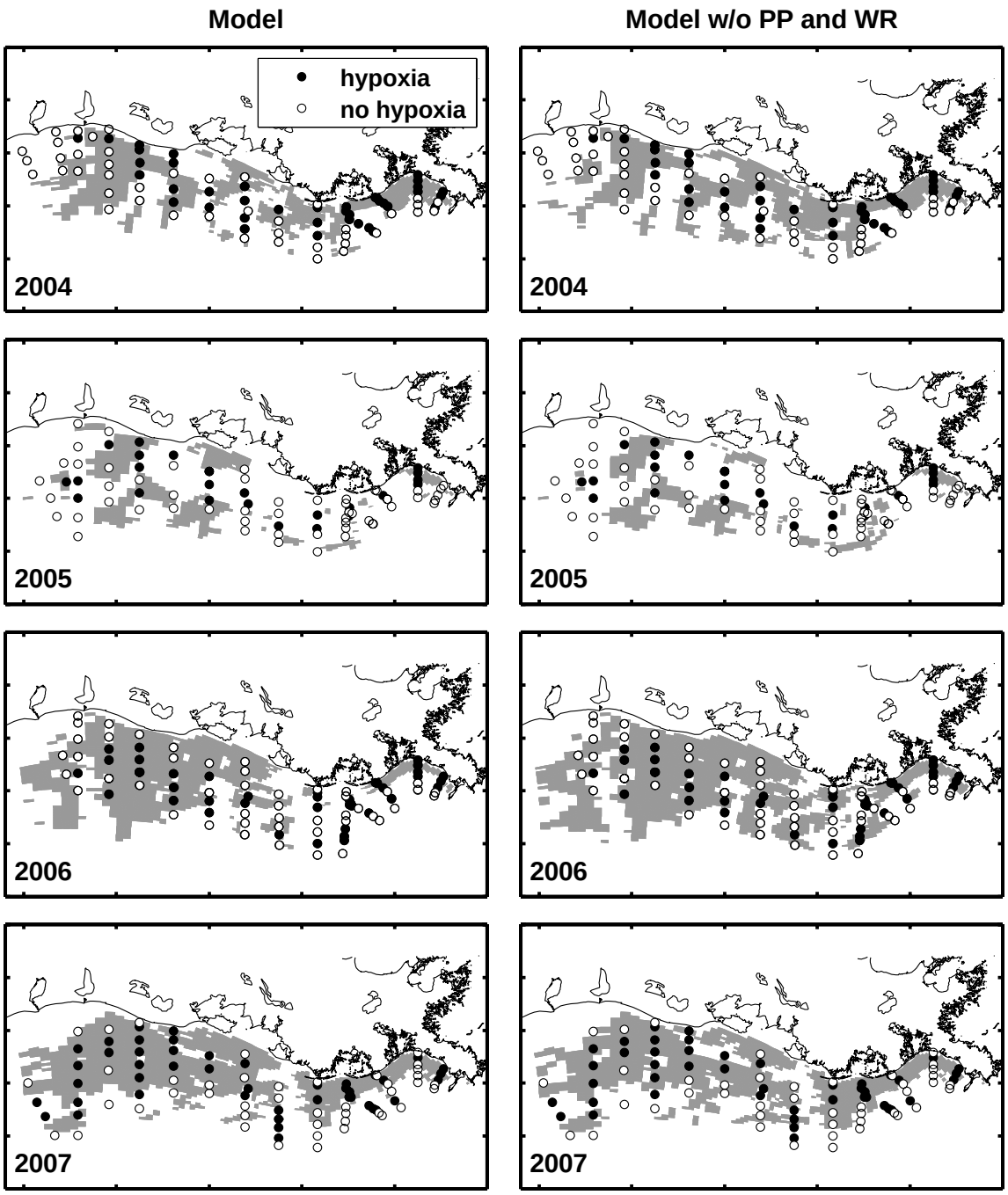

Fig. S2. Simulated (gray areas) and observed (dots) hypoxic conditions for the full model (left column) and the model without biological processes in water column (right column) for the years 2004 to 2007. The simulated hypoxic area includes all grid boxes where bottom water dissolved oxygen < 62.5 mmol/m^3 during the July monitoring cruise. The stations where hypoxia was observed are shown as filled black dots, while stations without hypoxia are shown as white dots.

II. Simulated oxygen budget and hypoxia by Model+CCR simulation

Table S3. Simulated 4-year (2004-2007) mean oxygen budget in summer for the four sub-regions by Model+CCR simulation. Oxygen source and sink terms are given for the surface layer above the pycnocline, for the mid layer and for the 5-m thick bottom layer.

Layers	O_2 flux	Mississippi Delta	Mississippi Intermediate	Atchafalaya Plume	Mid-shelf	All regions
	Airsea	-10.2	5.1	1.1	17.9	5.1
	PP	83.1	67.3	93.3	77.3	77.9
	WR	62.7	64.9	65.7	81.7	69.8
Surface	PP-WR	20.4	2.4	27.5	-4.3	8.1
	H+Vadv	-6.7	-2.9	-12.8	-11.9	-8.1
	Vdiff	-9.8	-11.4	-26.4	-12.3	-13.5
	Net	-6.2	-6.8	-10.5	-10.7	-8.4
	PP	64.7	54.6	44.0	61.1	57.4
	WR	83.7	64.3	45.1	81.2	71.4
Mid	PP-WR	-19.0	-9.7	-1.1	-20.1	-13.9
	H+Vadv	24.2	17.3	4.1	27.4	20.2
	Vdiff	-3.7	-7.8	1.7	-8.7	-5.8
	Net	1.5	-0.3	4.8	-1.4	0.5
	PP	13.6	19.6	23.9	8.7	15.4
	WR	21.6	26.7	43.1	18.8	25.4
	SOC	32.4	36.7	38.4	30.9	34.1
Bottom	PP-WR-SOC	-40.4	-43.8	-57.6	-41.1	-44.1
	H+Vadv	22.6	17.8	12.2	14.8	17.2
	Vdiff	13.6	19.2	24.7	21.0	19.3
	Net	-4.2	-6.8	-20.7	-5.3	-7.7

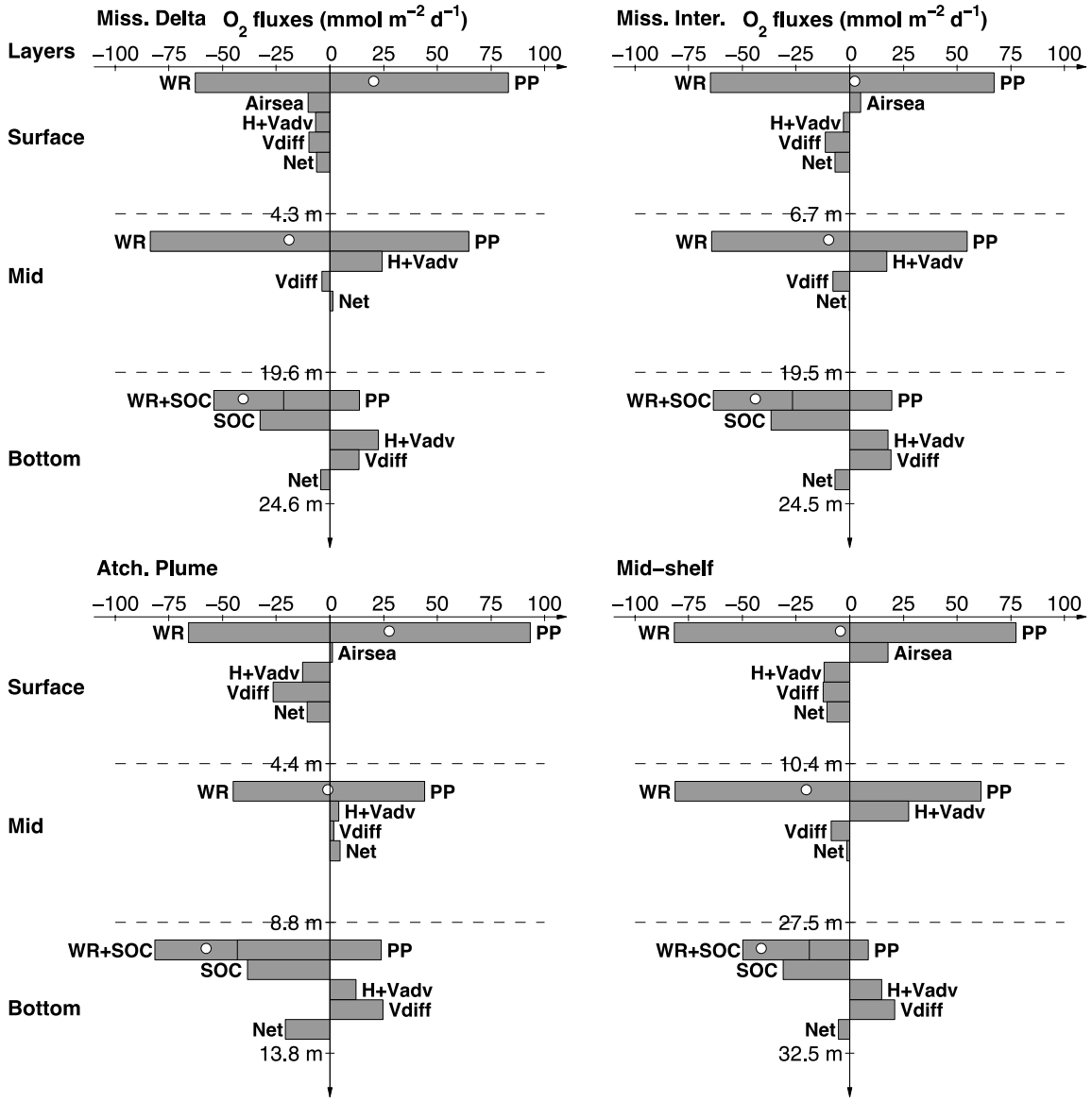

Fig. S3. Simulated 4-year (2004-2007) mean oxygen budget in summer for the 4 sub-regions by Model+CCR simulation. Oxygen source and sink terms are given for the surface layer above the pycnocline, for the mid layer and for the 5-m thick bottom layer. The average depth of the pycnocline, 5 m above bottom and the average water depth are indicated for each sub-region. The open circles indicate the balance of primary production and respiration in each layer. For the bottom layer, the bars for water column respiration (WR) and sediment oxygen consumption (SOC) are shown stacked and SOC is repeated separately.

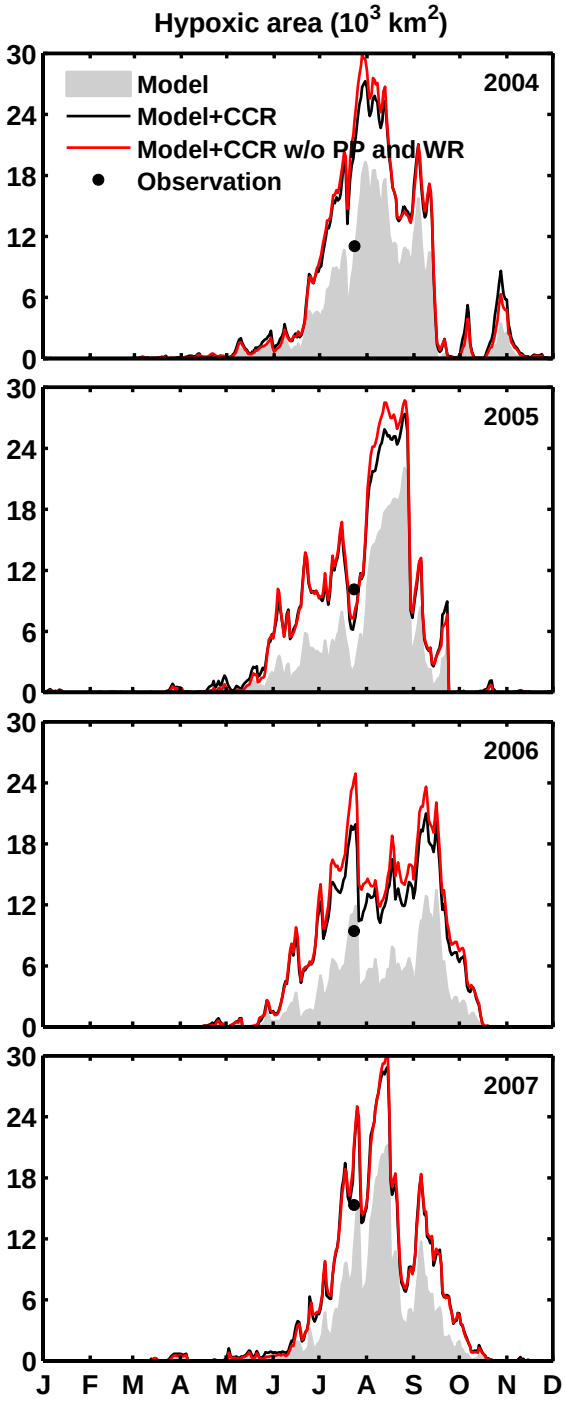

Fig. S4. Time series of simulated hypoxic extent for the normal model simulation (gray shadow), Model+CCR simulation (black line) and Model+CCR without biological processes in the water column (Model+CCR w/o PP and WR, red line). Also shown is the observed hypoxic extent in late July (black dots). The observed hypoxic extent was estimated by linearly interpolating the observed oxygen concentrations onto the model grid with Matlab's grid data function and then calculating the area with oxygen concentrations below the hypoxic threshold (Fennel et al., 2013).